International Journal of GEOMATE, Aug. 2023, Vol. 25, Issue 108, pp.21-29
ISSN: 2186-2982 (P), 2186-2990 (O), Japan, DOI: https://doi.org/10.21660/2023.108.3774
Geotechnique, Construction Materials and Environment

SPATIAL MODEL OF FLOOD HAZARD DUE TO LAND COVER CHANGE IN THE TARUSAN WATERSHED, WEST SUMATRA – INDONESIA

*Triyatno[1], Isril Berd[2] and Idris[3]

[1]Doctoral Program of Environmental Sciences-Universitas Negeri Padang, 25132, Indonesia
[2]Faculty of Agricultural Technology-Universitas Andalas, 25163, Indonesia
[3]Faculty of Economics-Universitas Negeri Padang, 25132, Indonesia

*Corresponding Author, Received: 29 Nov. 2022, Revised: 09 April 2023, Accepted: 23 April 2023

ABSTRACT:Spatial modeling of flood hazards in the Tarusan Watershed of West Sumatra has the objectives of modeling land cover changes from 2019-2029-2039, flood numerical models, and hybrid spatial models of flood hazards. The methods used in this research are quantitative methods and field surveys to determine the accuracy of the modeling results. The results showed that land cover changes in the Tarusan Watershed experienced a decrease in land cover changes, namely primary forest and secondary forest land cover, while a land cover that experienced an increase in area was oil palm land cover and fields. The numerical model of flooding in the Tarusan Watershed shows that the peak of the flood (Qp) takes 3.12 hours, the time required to reduce the flood discharge (Tp+0.3) is which is 7.69 hours, and the time required to reduce the flood discharge (Tp+0.3+1.5T0.3) is 14.54 hours. The results of the hybrid spatial modeling of flood hazards in the Tarusan Watershed from 2019 to 2039 have undergone extensive changes. Changes in the area affected by floods from 2019 to 2029 are 323.91 ha, and changes (prediction) in the area affected by floods from 2029 to 2039 are 242.58 ha Land cover changes from 2019 to 2029 affect flood discharge by 5.65%, and land cover changes from 2029 to 2039 affect flood discharge by 8.55%. For flood disaster mitigation efforts, it is necessary to have information to the community living in the Tarusan Watershed that a flood disaster will occur if the rainfall intensity is more than 50 mm/hour with a duration of 1.11 hours, then the time needed to reach the peak of the flood is 3.12 hours, so that the community can anticipate the losses that will arise from the flood disaster

Keywords: Land cover, Flood hazard, Spatial models

1. INTRODUCTION

Recent climate change often triggers natural disasters such as landslides, floods, flash floods, and droughts [1-4]. The increasing intensity of natural disasters is inseparable from human behavior toward the environment. Humans to meet their needs often make changes to the environment [5,6]. This causes changes in the environmental response to natural phenomena that occur [7-9]. Human activities to meet their daily needs often make changes to land cover which will have an impact on microclimate changes due to the reduction in the area of primary and secondary forests [10,11]. Reduction of forest area will have an impact on the environment such as changes in micro temperature, disruption of the existing water balance in a watershed, and in the end, will have an impact on natural disasters such as landslides, floods, flash floods, and droughts [12-15].

One of the areas experiencing changes in landcover is the Tarusan Watershed. Changes in land cover, especially in the upstream part of the watershed, cause the soil's ability to absorb water to be smaller and the run off will be greater, this is one of the triggers for flooding in addition to the global anomaly climate factor.

Tarusan Watershed is located on the coast of West Sumatra Province which connects the cities of Padang and Painan and Bengkulu Province. One of the impacts of land cover changes in the Tarusan Watershed is flood disasters such as those that occurred on December 30, 2012 and May 17, 2017 with flood water levels reaching 50 cm to 150 cm. Floods in the Tarusan Watershed often have an impact on the community, namely the inundation of settlements and agricultural land which causes crop failure and congestion for up to nine hours. The impact of congestion disrupts access from Padang City to the capital of the Pesisir Selatan Regency, namely Painan, and Bengkulu Province, especially for the distribution of economic goods.

Given the importance of land cover in a watershed as a control of environmental balance [16-18], researchers want to analyze and model changes in land cover and their effect on flood discharge that occurs in the Tarusan Watershed. The numerical model in this research is designed to determine the value of the effect of land cover change on flood discharge, as well as determine the time of occurrence of the peak flood discharge and the time it takes until the flood discharge recedes. This information is very important in flood mitigation efforts, so that losses from flood disasters in the Tarusan Watershed, both property and human life losses can be reduced. The importance of research on land cover change models and their effect on changes in flood discharge in the Tarusan Watershed, will provide important information to local governments and communities living in the Tarusan Watershed which can be seen in the research significance

2. RESEARCH SIGNIFICANCE

Reducing the area of the forest will have an impact on the environment. One of the impacts of land cover change is that it will result in increased flood discharge. In this case, the significance of the study is to produce an e-numerical model of flood disasters in the Tarusan Watershed that has flood characteristics quickly and produce a land cover change model that determines changes in flood discharge from 2019 to 2039 spatially which is useful for formulating policies that regulate land cover change, especially in the upstream part of the Tarusan Watershed and as information for local governments and communities living in the Tarusan Watershed for increase flood mitigation efforts.

3. METHODS

The method used for modeling land cover change and flood modeling is quantitative. The stages carried out in this modeling are preparation, modeling, model interpretation, and modeling accuracy test. To do land cover change modeling and flood modeling some data are needed, as shown in Table 1 below.

Table 1 Required data

Data	Uses
Landsat of 5 (2000), Landsat of 7 (2009), Landsat of 8 (2019) in USGS	Land cover in 2000, Land cover in 2009, Land cover in 2019
Indonesia's National Seamless Digital Elevation Model (DEM) 2022	3D Modeling for hybrid spatial models of flood
Rain data (2009-2019) in Office of Water Resources Management, West Sumatra Province	Numerical model of flood discharge

3.1 Analysis Model of the Land Cover Change

To determine the land cover change model, the Marcov chain Celluler Automata formula [19] is used which uses the assumption that future land cover changes $_{xt}$ +1, and ($_t$+1) depend on current conditions expressed by$_{xt}$.To determine the transition matrix for land cover change, the formula proposed by [20,21] as follows:

$$P = (pij) = \begin{matrix} P1.1p1.2p1.n \\ p2.1p2.2p2.n \\ Pn.1pn.2pn.n \end{matrix} \quad (1)$$

The above formula for determining the transition matrix for land cover change can be simplified as follows.

$$P(n) = p\,(n-1)\,pij \quad (2)$$

3.2 The Model of Carrying Out Flood Disaster

In carrying out flood disaster modeling, it is done by determining the return period of rain, design discharge, and numerical model of Nakayasu Synthetic Unit Hydrograph (HSS) [16, 22]. The rainfall return period was determined using a Pearson type III log [17,23].

3.2.1 Pearson type III logs

To determine the design rain using the Log Pearson type III method, the formula proposed by [23,24] is used as follows:

$$LogXTr = LogX + KTr * (Slogx) \quad (3)$$

$Log\ XT$ = the amount of planned rainfall for the return period T years

$Log\ X$ = average value of data.

$$\sum_{i=n}^{n} \frac{Logxi}{n} \quad (4)$$

Slog x = standard deviation.

$$Sx = \sqrt{\frac{\sum_{i-1}^{n}(Logxi - Logx)^2}{n-1}} \quad (5)$$

KTr = frequency coefficient, which is obtained based on the relationship between the value of Cs and the return period T.

$$Cs = \frac{\sum_{i-1}^{n}(Logxi - Logx)^2}{(n-1)(n-2).(SLogx)^2} \quad (6)$$

$$(x)^2\,hit = \sum_{n=1}^{k} \frac{EF - OF)^2}{EF} \quad (7)$$

$$EF = \frac{n}{k} \quad (8)$$

Where:

$(x)^2\,hit$ = test statistic

OF = observed value (observed frequency)

EF = expected value (expected frequency)

Smirnov Kolmogorov test (horizontal data test) is used to test the horizontal deviation [5,25] using the following formula.

$$\Delta\, maks\ [(PE\ (x) - Pt\ (x)] \tag{9}$$

Where:
$maks$ = difference between theoretical and empirical probability data
$Pt\ (x)$ = data position x according to the theoretical distribution
$PE\ (x)$ = data position x according to empirical distribution.

3.2.2 Plan debit/maximum debit

$$Qp\ =\ 0{,}00278.CIA \tag{10}$$

Where:
Qp = peak discharge (m³/s)
C = runoff coefficient
I = rain intensity with flood concentration time (mm/hour)
A = area of the river basin (ha)

3.2.3 Rain intensity

To determine the amount of rain intensity, the Mononobe method [24] the following:

$$I = (\frac{R_{24})}{24} \frac{(24)^{2/3}}{t} \tag{11}$$

Where:
I = rain intensity
R_{24} = maximum daily rainfall (mm)
t = time of rainfall (hours)

Synthetic unit hydrograph Nakayasu method [22] using the formula.

Tg = 0,4 + 0,058 $.L$
A = 0,47.$(AL)^{0{,}25\ \mathrm{Tg}}$
Tp = Tg +0,8.Tr
$T0{,}3$ = $\alpha.Tg$

To determine the ascending curve of the Nakayasu synthetic unit hydrograph [22], the following formula is used.

$$Q\alpha = Qp.\left(\frac{t}{Tp}\right)^{2.4} \tag{12}$$

To determine the value of the synthetic unit hydrograph [22], the following formula is used.

$$Q_{d1} > 0{,}3Qp\ Q_{d1} = Qp.0{,}3 \wedge \left(\frac{t-Tp}{T0{,}3}\right) \tag{13}$$

$$0{,}3Qp > Q_{d2} > 0{,}3^2 Qp Q_{d2} = Qp.0{,}3 \wedge \left(\frac{t-Tp+0{,}5\ T0{,}3}{1{,}5\ T0{,}3}\right) \tag{14}$$

$$0{,}3^2 Qp > Q_{d3}\ Q_{d2} = Qp.0{,}3\ \left(\frac{t-Tp+1{,}5\ T0{,}3}{2{,}0\ T0{,}3}\right) \tag{15}$$

Where:
Qp = peak discharge (m³/s)
Ro = unit rain (mm)
Tp = time of peak flood (hours)
Tr = duration of rain
= coefficient of rainwater runoff
$T0.3$ = time needed to reduce flood discharge from Qp to 0.3 Qp
Tp = Tg.0,8Tr
L< 15 km tg = 0.21.L 0.7
L> 15 km tg = 0.4 +0.058.L
L = length of main river
Tg = concentration time (hours)
Tr = 0.5 tg to tg (hours)
$T0.3$ = $.tg$ (hours)
= 0.47.$A.L$ 0.25/tg
= 2 for ordinary watershed
= 1.5 for the slow ascending hydrograph

3.3 The hybrid spatial model of flood hazard

To determine the hybrid spatial model of flood hazard, the multiple criteria analysis is used with the formula proposed by [25-27] as follows.

$$FHM = 0.1 * GL + 0.1 * GM + 0.1 * T + 0.15L + 0.15CH + 0.1Pl + 0.3 * ID \tag{16}$$

Where:
GL = geology
GM = geomorphology
T = soil type
L = slope class
CH = rainfall
PL = land cover and land cover
ID = inundation

To determine whether the modeling results are acceptable or not, it is necessary to test the modeling accuracy using user accuracy, producer accuracy, and overall accuracy, using the formula proposed by [22,28] as follows.

$$Useraccuracy = \frac{xii}{x+1} * 100\% \tag{17}$$

$$Produceraccuracy = \frac{Xii}{Xi+1} * 100\% \tag{18}$$

$$Overallaccuracy = \frac{\sum_i^r xii}{N} * 100\% \tag{19}$$

Where:
Xii = the diagonal values
Xi = the number of pixels in the i_th row
$X + i$ = the number of pixels in the i_th column
N = many pixels in the sample

4. RESULTS

4.1 Model Results of the Land Cover Change

Table 2 Land Cover change model from 2019-2039

Land cover	2019			2029			2039		
	Pixel	Large (ha)	(%)	Pixel	Large (ha)	(%)	Pixel	Large (ha)	(%)
Primery forest	168.437	15.159,33	53,45	162.499	14.624,91	51,57	152.132	13.691,88	48,28
Secondary forest	63.372	5.703,48	20,11	55.788	5.020,92	17,7	46.286	4.165,74	14,69
Palm Oil	38	3,42	0.01	9.000	810	2,86	27.308	2.457,72	8,67
Mangrove	40	3,6	0.01	40	3,6	0,01	40	3,6	0,01
Water body	2.494	224,46	0,79	2.494	224,46	0,79	2.494	224,46	0,79
Build-up/Settlements	11.027	992,43	3,5	11.071	996,39	3,51	11.085	997,65	3,52
Paddy field	15.379	1.384,11	4,88	15.373	1.383,57	4,88	15.373	1.383,57	4,88
Dry land farming	1.755	157,95	0,56	14.446	1.300,14	4,58	21.986	1.978,74	6,98
Mixed gardens	52.587	4732,83	16,69	44.418	3.997,62	14,1	38.425	3.458,25	12,19
Total	315.129	28361,61	100	315.129	28.361,61	100	315.129	28.361,61	100

Source: Data analysis 2022

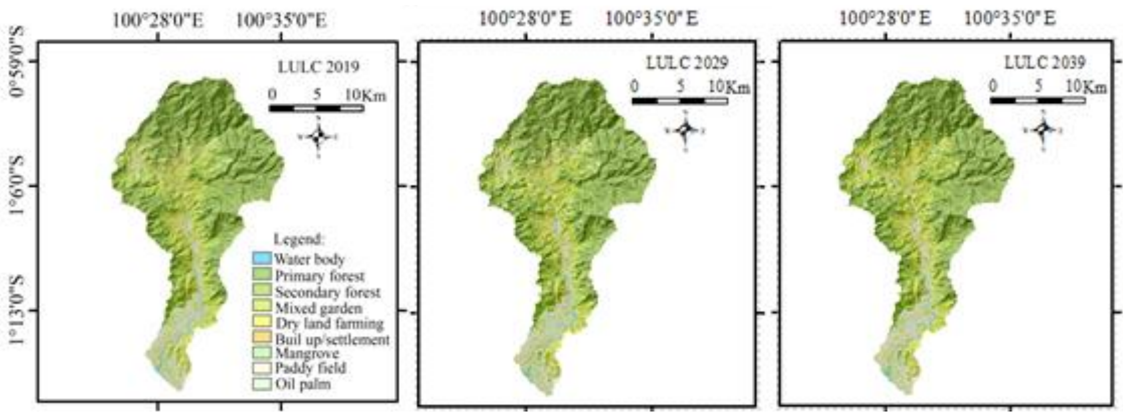

Fig.1 Model Map of land cover change for 2019, 2029, and 2039.

The land cover change model was obtained using a driving force, including slope, elevation, distance from the road, distance from health facilities, distance from government center, and distance from educational facilities. The closer to health facilities, education, and maintenance centers, the distance from the road, the more land cover changes, and the higher the elevation and steeper slopes, the less land cover changes. The results of the modeling of land cover changes in the Tarusan Watershed can be seen in Table 2, and Fig 1 above. For Table 2 above shows that primary forest land cover experienced the most changes, namely for 2019, 2029, and 2039. The amount of change in the primary forest from 2019, and to 2029 was 534.42 ha or 1.88%, while the change in primary forest land cover from 2019 2029 to 2039 there will be a change of 933.03 ha or 3.29%.

Another land cover that experienced a reduction in the area was secondary forest, where the change in secondary forest land cover area from 2019 to 2029 was 682.56 ha or 2.41%, and changes in secondary forest land cover from 2029 to 2039 were 855.18 ha or 3.01%. More details can be seen in the following Fig 2 below

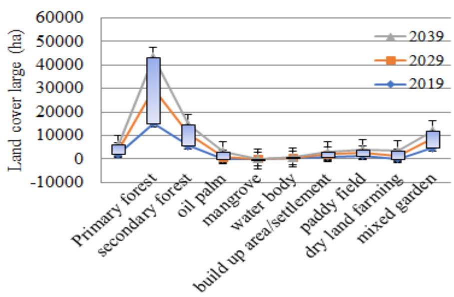

Fig. 2 Graph of land cover change from 2019 to 2039

The change in land cover that experienced the most extensive increase from 2019 to 2039 was oil palm land cover, where oil palm land cover increased in area from 2019 to 2029 covering an area of 806.58 ha or 2.85%, and from 2029 to 2039 the area oil palm land cover increased by 1647.72 ha or 5.81%. Another land cover that experienced an increase in area was the land cover of fields, where the area of field land cover in 2019 to 2029 experienced an increase in the area of 1142.19 ha or 4.02%, while from 2029 to 2039 the land cover of fields experienced an increase in the area of 678,6 ha or 2.4%.

4.2 Model Results of the Carrying Out Flood

To determine the return period of rain for 100 years used the Log Pearson type III method which can be seen in Table 3. Where Table 3 shows that the planned rainfall for a return period of 100 years is in the Tarusan Watershed, where the lowest rainfall is 142.75 mm and the highest planned rainfall is 234.78 mm. The suitability test of the method was carried out before calculating the flood discharge, where the results of the calculation of the method obtained suitability a *T-table* value of 0.32 and a *T-table* value of 0.62, thus the Log Pearson type III method can be said to be suitable for predicting flood discharge in the research area. To determine the planned discharge in the Tarusan Watershed, the author uses the Log Pearson type III method. Before determining the design discharge, it is necessary to know the rain intensity, the coefficient value of drainage, and the watershed area. More details can be seen in the following Fig 3 and Table 3 below.

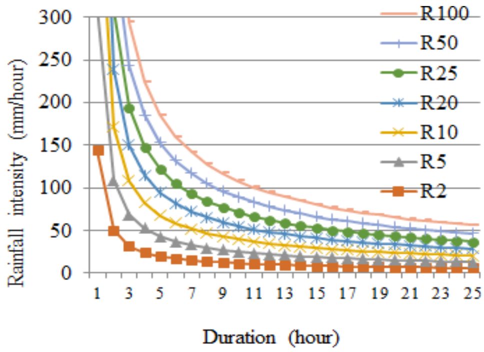

Fig. 3 Graph of rain intensity with 100 year return period

Fig 3 above shows the highest value of rainfall intensity in the Tarusan Watershed, which is 81.43 mm/hour and the lowest is 6.01 mm/hour. The value of rain intensity will affect the amount of flood discharge in the Tarusan Watershed. Another factor influencing flow rate is the magnitude of the flow coefficient value which is influenced by land cover in watershed. The flow coefficient values in the Tarusan Watershed due to land cover changes can be seen in the following Table 4 below.

Table 3 Rain return period of the Pearson method Type III

Return period	Log Average	Ktr	*S Log*X	Rainfall plan
2	2,16	-0,014	0,075	144,176
5	2,16	0,837	0,075	168,648
10	2,16	1,2	0,075	180,325
20	2,16	1,588	0,075	193,714
25	2,16	1,783	0,075	200,777
50	2,16	2,36	0,075	223,327
100	2,16	2,628	0,075	234,646

Source: Data analysis 2022.

Table 4 Value of the Tarusan Watershed flow coefficient in 2019, 2029, and 2039

Land cover	*C* 2019	(%) Large 2029	*C* 2029	(%)Large2039	*C* 2039
Primery forest	0,011	0,515	0,010	0,483	0,009
Secondary forest	0,006	0,177	0,005	0,147	0,004
Palm Oil	0,000	0,028	0,003	0,087	0,008
Mangrove	0,000	0,001	0,000	0,000	0,001
Water body	0,000	0,007	0,000	0,008	0,004
Build-up/Settlements	0,010	0,035	0,011	0,035	0,010
Paddy field	0,007	0,048	0,007	0,049	0,007
Dry land farming	0,001	0,045	0,005	0,070	0,006
Mixed gardens	0,017	0,140	0,014	0,122	0,012
Total	0,052	1,000	0,055	1,000	0,060

Source: Data analysis 2022.

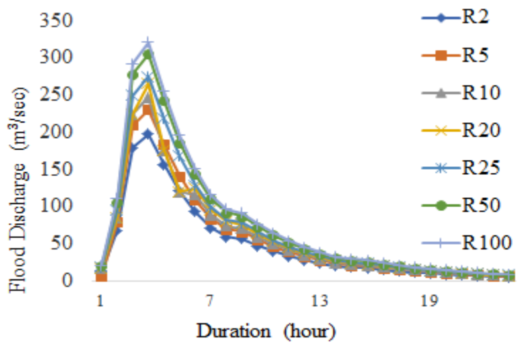

Fig. 4 Flood discharge hydrograph model

Fig 4 and Table 4 above shows that land cover changes influence the flow coefficient values in the Tarusan Watershed. The flow coefficient value in 2019 is 0.052, in 2029 the flow coefficient value changes to 0.055, and in 2039 the flow coefficient value is 0.060.This change in the coefisen value of the flow is caused by changes in land cover, where changes in the flow coefficient values from 2019 to 2029 will affect the flood discharge by 5.65% and the change in the flow coefficient values from 2029 to 2039 will affect the flood discharge by 8.55%. The peak flood discharge (Tp) occurred at 3,120 hours, and the flood discharge decreased by Tp. 0.3 occurred at 7.69 hours, and a decrease in flood discharge of (Tp+T0.3+1.5T0.3) occurred at 14.54 hours. Where also has flood characteristics that quickly reach the peak of the flood and quickly reach normal discharge.

4.3 Model Results of The Hybrid Spatial of Flood

The hybrid spatial model results of flooding in the Tarusan Watershed in 2019 are the area that has a low flood hazard of 25,539.98 ha or 90.05%, a medium hazard of 2,728.785 ha or 9.62%, and a high flood hazard of 92.83 ha or 0.32%. The area of flood hazard in 2029 is an area that has a low flood hazard of 24,273.41 ha or 85.58%, a medium flood hazard of 3,671.45 ha or 12.94%, and a high flood hazard of 416,74 ha or 1.469%.

The flood hazard in 2039 has different from previous years, especially in terms of area. The area of low flood hazard in 2039 is 24.73.06 ha or 87.21%, the medium hazard is 2,968.22 ha or 10.46%, and the high hazard is 659.32 ha or 2.32%. The hybrid spatial modeling results of flood hazards in the Tarusan Watershed from 2019 to 2039, show that there is a change in the area affected by flood hazards, especially in areas that have high hazards. The area of high flood hazard from 2019 to 2029 experienced an increase in the area of 323. 91 ha, and from 2029 to 2039 there was an increase in the area affected by flooding by 242.57 ha. The hybrid spatial model results of flooding need to be tested for accuracy to determine whether the modeling results are acceptable or not. More details can be seen in Table 5-7, and for more details, the flood model in the Tarusan Watershed in 2019, 2029, 2039 and the hybrid spatial model (Fig 5) are below.

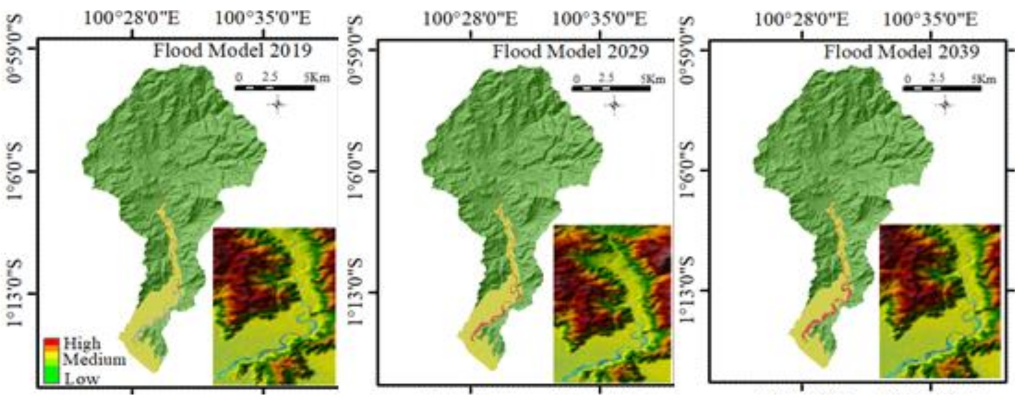

Fig. 5 Flood hazard spatial model for 2019, 2029, 2039 and map of hybrid spatial model of flood hazards

Table 5 Accuracy test of the 2019 flood hazard model

Flood hazard	Low	Medium	High	User Accuracy
Low	172	5	4	94.50
Medium	6	187	7	93.50
High	0	1	16	94.12
Producer Accuracy	96.63	96.89	59.25	-
Overall Accuracy	172+187+16=375/399			93.98

Source: Data analysis 2022.

Table 6 Accuracy test of the 2029 flood hazard model

Flood hazard	Low	Medium	High	User Accuracy
Low	169	7	6	92.85
Medium	10	183	7	91.50
High	0	2	15	88.23
Producer Accuracy	94.41	95.31	53.57	-
Overall Accuracy	169+183+15=367/399			91.98

Source: Data analysis 2022.

Table 7 Accuracy test of the 2039 flood hazard model

flood hazard	Low	Medium	High	User Accuracy
Low	165	9	8	90.66
Medium	10	183	7	91.50
High	1	2	14	82.35
Producer Accuracy	93.75	94.33	48.28	-
Overall Accuracy	165+183+14=362/399			90,73

Source: Data analysis 2022.

Testing the accuracy of the hybrid spatial model for flood disaster in the Tarusan Watershed using overall accuracy, the accuracy value of the hybrid spatial model for flood disaster in 2019 was 93.98, in 2029 it was 91.98, and in 2039 the overall accuracy value was 90.73. Based on the results of the accuracy test of the hybrid spatial model of flooding in the Tarusan Watershed using overall accuracy, it can be said to be good, so it can be said that the results of the hybrid spatial modeling of floods in the Tarusan Watershed are acceptable.

5 CONCLUSIONS

Based on the research results above, it can be concluded as follows 1) The land cover change model in the Tarusan Watershed has changed, especially in primary forest and secondary forest land cover experiencing a decrease, while oil palm land cover have increased in the area; 2) The numerical model of the flood disaster in the Tarusan Watershed has the characteristics of flooding that occurs quickly and quickly also experiences a reduction in flood discharge; 3) The hybrid spatial model of flood hazard in the Tarusan Watershed underwent extensive changes from 2019 to 2039.

6 ACKNOWLEDGMENTS

This paper is written as a condition for running the exam for the author's dissertation in the Doctoral Program of Environmental Sciences, Postgraduate School-Universitas Negeri Padang. The author would like to thank the Pesisir Selatan Regency Government, especially for his ideas, data, and information for my dissertation.

7 REFERENCES

[1] Acuna-Alonso C., Novo, A., Rodríguez, J.L., Varandas, S., and Álvarez, X., Modelling and evaluation of land use changes through satellite images in a multifunctional catchment: Social, economic and environmental implications. Ecological Informatics, Vol. 71, 2022, pp. 1-15.

[2] Donovan M., Modelling soil loss from surface erosion at high-resolution to better understand sources and drivers across land uses and catchments; a national-scale assessment of Aotearoa, New Zealand. Environmental Modelling and Software, Vol. 147, 2022, pp. 105228.

[3] Dahri N., and Abida H. Hydrologic modeling and flood hydrograph reconstitution under an arid climate condition: case of Gabes Watershed, South-Eastern Tunisia. Environment, Development and Sustainability, Vol. 24, 2022, pp. 1-20.

[4] Bertsch R., Glenis, V., and Kilsby C., Building level flood exposure analysis using a hydrodynamic model. Environmental Modelling and Software, 156, 2022, pp. 1-8.

[5] Sulong S., and Romali N.S., Flood Damage Assessment: a Review of Multivariate Flood Damage Models. International Journal of GEOMATE, Vol. 22, Issue. 93, 2022, pp. 106-113.

[6] Savitri Y.S., Kakimoto R., Anwar, N.,Wardoyo W., and Suryani, E., Reliability of 2d Hydrodynamic Model on Flood Inundation Analysis. International Journal of

GEOMATE, Vol. 21, Issue. 83, 2021, pp 65-71.
[7] Wang Z., Shu L., Xu P., Yin X., Lu C., Liu B, and Li Y., Influence of land use changes on the remaining available aquifer storage (RAAS): A case study of the Taoerhe alluvial-proluvial fan. Science of the Total Environment, Vol. 849, 2022, pp. 1-13.
[8] Li Z., Chen M., Gao S., Wen Y., Gourley J.J., Yang T., and Hong Y., Can re-infiltration process be ignored for flood inundation mapping and prediction during extreme storms? A case study in Texas Gulf Coast region. Environmental Modelling and Software, Vol. 155, 2022, pp.1-14.
[9] Wu J., Luo J., Zhang H., Qin S., and Yu M., Projections of land use change and habitat quality assessment by coupling climate change and development patterns. Science of the Total Environment, 847, 2022, pp. 1-12.
[10] Rigby A.M.F., Butcher P.W.S., Ritsos P.D., and Patil S.D., LUCST: A novel toolkit for Land Use Land Cover change assessment in SWAT+ to support flood management decisions. Environmental Modelling and Software, Vol. 156, 2022, pp.1-12.
[11] Molter A., and Lindley S., Developing land use regression models for environmental science research using the XLUR tool-More than a one-trick pony. Environmental Modelling and Software, Vol.143, 2021, pp.1-11.
[12] Huang Y.H., Mirzaei M., and Yap W.K.,Flood Analysis in Langat River Basin Using Stochatic Model. International Journal of GEOMATE, Vol. 11, Issue, 27, 2021, pp. 2796–2803.
[13] Zhang P., Cai Y., He Y., Xie Y., Zhang X., and Li Z., Changes of vegetational cover and the induced impacts on hydrological processes under climate change for a high-diversity watershed of south China. Journal of Environmental Management, Vol. 322, 2022, pp.1-12.
[14] Triyatno., Bert I., Idris., Hermon D., and Putra A., Hazards and Morphometry to Predict the Population Loss Due of Landslide Disasters in Koto XI Tarusan-Pesisir Selatan. International Journal of GEOMATE, Vol. 19, Issue, 76, 2020, pp. 98–103.
[15] Agonafir C., Lakhankar T., Khanbilvardi R., Krakauer N., Radell, D., and Devineni, N., A machine learning approach to evaluate the spatial variability of New York City’s 311 street flooding complaints. Computers, Environment and Urban Systems, Vol. 97,2022, pp.1-11.
[16] Romali N.S.,Yusop Z., and Ahmad Zuhdi Ismail., Application of Hec-ras and Arc GIS for Floodplain Mapping in Segamat Town, Malaysia. International Journal of GEOMATE, Vol. 15, Issue. 47, 2021, pp. 7–13.
[17] Hang H.T., Hoa P.D., Tru V.N., and Phuong, N.P., Application of Shannon’s Entropy Model and GIS in Flash Flood Forecasting Along National Highway-6, Hoa Binh Province, Vietnam. International Journal of GEOMATE, 21(87), 2021, pp. 50–57.
[18] García-Alén G., González-Cao J., Fernández-Nóvoa D., Gómez-Gesteira M., Cea, L., and Puertas J., Analysis of two sources of variability of basin outflow hydrographs computed with the 2D shallow water model Iber: Digital Terrain Model and unstructured mesh size. Journal of Hydrology, Vol. 612,2022, pp.1-12.
[19] Kesuma T.N.A., Kusuma M.S.B., Farid M., Kuntoro A.A., and Rahayu, H.P., An Assessment of Flood Hazards Due to the Breach of the Manggarai Flood Gate. International Journal of GEOMATE, Vol. 23, Issue. 95, 2022, pp. 104–111.
[20] Hoshino T., and Yamada T.J., Spatiotemporal classification of heavy rainfall patterns to characterize hydrographs in a high-resolution ensemble climate dataset. Journal of Hydrology, Vol. 617, 2023, pp.1-8**.**
[21] Mitiku A.B., Meresa G.A., Mulu T., and Woldemichael A.T., Examining the impacts of climate variabilities and land use change on hydrological responses of Awash River basin, Ethiopia. Hydro Research, Vol. 6, 2023, pp. 16-28.
[22] Dewata I., and Umar I., Management of Flood Hazard Areas in Pasaman River Basin of West Pasaman Regency West Sumatra Province. International Journal of GEOMATE, Vol. 17, Issue. 64, 2019, pp. 230-237.
[23] Hooker H., Dance S.L., Mason D.C., Bevington, J., and Shelton, K., Spatial scale evaluation of forecast flood inundation maps. Journal of Hydrology, Vol. 612, 2022, pp. 1-14.
[24] Garciano L.E., Tanhueco R.M., Torres A., and Iguchi H., Assessing Vulnerabilities and Costs of Power Outages to Extreme Floods in Surigao City, Philippines. International Journal of GEOMATE, Vol. 20, Issue. 82, 2021, pp. 7-14.
[25] Istijono B., Putra T.H.A., Rusman B., and Ophiyandri, T., The Dynamics of Land Cover Change And Causal Factors In The Kuranji Watershed. International Journal of GEOMATE, Vol. 21, Issue. 84, 2021, pp. 69-75.
[26] Ismail M.S.N., Ghani A.N.A., and Ghazaly Z.M., The characteristics of road inundation

during flooding events in peninsular Malaysia,International Journal of GEOMATE, Vol. 16, Issue. 54, 2019, 129-133.

[27] Taniguchi K., Kotone K., and Shibuo Y., Simulation-based assessment of inundation risk potential considering the nonstationarity of extreme flood events under climate change. Journal of Hydrology, Vol. 61, 2022, pp. 1-15.

[28] Ngo H., Bomers A., Augustijn D.C., Ranasinghe, R., Filatova, T., van der Meulen, B., and Hulscher S.J., Reconstruction of the 1374 Rhine river flood event around Cologne region using 1D-2D coupled hydraulic modelling approach. Journal of Hydrology, Vol. 617, 2023, pp. 129039.